

Article

## Preparation of Thermo-Responsive Poly(ionic liquid)s-Based Nanogels via One-Step Cross-Linking Copolymerization

Jing Zhang <sup>1</sup>, Jingjiang Liu <sup>1</sup>, Yong Zuo <sup>1</sup>, Rongmin Wang <sup>1</sup> and Yubing Xiong <sup>1,2,\*</sup>

<sup>1</sup> Key Laboratory of Eco-Environment-Related Polymer Materials, Ministry of Education; College of Chemistry and Chemical Engineering, Northwest Normal University, Lanzhou 730070, China; E-Mails: zhang\_jing1121@163.com (J.Z.); liujingjiang214@163.com (J.L.); zuoyong\_only@163.com (Y.Z.); wangrmcn@163.com (R.W.)

<sup>2</sup> Max Planck Institute for Polymer Research, Ackermannweg 10, Mainz 55128, Germany

\* Author to whom correspondence should be addressed; E-Mail: xiongyb@mpip-mainz.mpg.de or yubing\_xiong@163.com; Tel.: +86-931-797-0358; Fax: +86-931-797-0075.

Academic Editor: Jason P. Hallett

Received: 11 August 2015 / Accepted: 14 September 2015 / Published: 18 September 2015

**Abstract:** In this study, thermo-responsive polymeric nanogels were facilely prepared via one-step cross-linking copolymerization of ethylene glycol dimethacrylate/divinylbenzene and ionic liquid (IL)-based monomers, 1,*n*-dialkyl-3,3'-bis-1-vinyl imidazolium bromides ([C<sub>*n*</sub>VIm]Br; *n* = 6, 8, 12) in selective solvents. The results revealed that stable and blue opalescent biimidazolium (BIm)-based nanogel solutions could be obtained without any precipitation when the copolymerizations were conducted in methanol. Most importantly, these novel nanogels were thermo-response, and could reversibly transform to precipitation in methanol with temperature changes. Turbidity analysis and dynamic light scattering (DLS) measurement illustrated that PIL-based nanogel solutions presented the phase transform with upper critical solution temperature (UCST) in the range of 5–25 °C. The nanogels were characterized using Fourier transform infrared (FTIR), thermogravimetric analyses (TGA), and scanning electron microscopy (SEM). In addition, BIm-based nanogels could also be used as highly active catalysts in the cycloaddition reaction of CO<sub>2</sub> and epoxides. As a result, our attributes build a robust platform suitable for the preparation of polymeric nanomaterials, as well as CO<sub>2</sub> conversion.

**Keywords:** ionic liquids; thermo-response; nanogels; cross-linking polymerization; UCST; CO<sub>2</sub> conversion

## 1. Introduction

In the past few decades, ionic liquids (IL) have garnered considerable attention in a variety of fields because of their excellent properties, such as vanishingly low vapor pressure, non-flammable, excellent chemical and thermal stability in the liquid state, polarity tunability, high ionic conductivity, wide electrochemical windows, *etc.* [1–6]. Meanwhile, poly(ionic liquid)s (PILs), derived from the polymerization of IL-based monomers and regarded as a distinct subclass of polyelectrolytes, can combine some unique characters of ILs with the practical properties of polymers, including processability, durability, mechanical stability. Therefore, PILs have also been collecting more and more interests in the fields of solid ion conductors, CO<sub>2</sub> sorbents, dispersants, porous materials, carbon precursors, potential desalination applications, *etc.* [7–11].

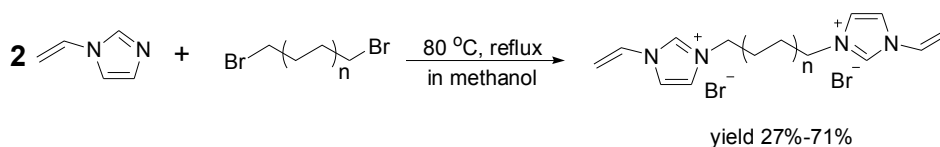
Recently, IL-derived stimuli-responsive systems, especially thermo-responsive behavior in different solvents, have been extensively investigated and considered as one of the promising “intelligent” materials [12–16]. In general, thermo-responsive phase behaviors of the polymer/solvent mixtures can be divided into two general classes: that with an upper critical solution temperature (UCST) and that with a lower critical solution temperature (LCST) depending on mixing behavior of the corresponding polymer solutions upon temperature change. To date, the fabrication of IL-based thermo-responsive phase behaviors can be achieved through IL/molecule liquid mixture, polymer/IL mixture, and homo-/copolymerization of IL. Several latest reviews have summarized the recent development on the design of ILs/PILs with thermo-responsive phase behaviors in water and organic solvents [17–19]. As cited in these reviews, some interesting thermo-responsive IL/PIL systems were masterly explored. Both H. Ohno and J. Yuan groups have contributed great in this field [20–23]. In brief, the origin of the thermo-responsive phase behavior of ILs/PILs was inherently derived from the non-covalent interactions between IL and solvents. Given the structural diversity of the component ions, there are still many promising PIL materials that have great potential to present the thermo-responsive phase behavior. Moreover, these thermo-responsive PIL materials will provide the opportunity for discovering unprecedented phenomena and applications not previously realized for the classical neutral thermo-responsive polymers [24,25].

More recently, our group has demonstrated a facile synthesis strategy to prepare PIL-based nanogels via the conventional radical copolymerization of IL-based monomers and the cross-linkers ethylene glycol dimethacrylate (EGDMA) and divinylbenzene (DVB) in selective solvents [26,27]. Interestingly, thermo-responsive nanogels could be obtained for the first time via the copolymerization of the geminal dicationic, 1,4-butanediyl-3,3'-bis-1-vinyl imidazolium halides, and the cross-linkers described previously under the same conditions [28]. These novel PIL-based thermo-responsive nanogels can reversibly form precipitates or macrogels in methanol with the temperature changing in the range of –15 to 25 °C. Experimental studies revealed that the thermo-response of PIL-based nanogels was attributed to hydrogen bonding interactions between nanogels and methanol. Unfortunately, this strategy is infeasible when it comes to ILs which cannot form hydrogen bonding [26,27]. Thus, it is highly desired to get insight into the rules of the thermo-responsive behavior, and develop a simple approach for the preparation of thermo-responsive nanogels based PIL. To achieve this goal, we will elucidate the relationship between the thermo-response of nanogels and the structure of ionic liquid-based monomers in this paper.

## 2. Results and Discussion

### 2.1. Synthesis of Biimidazolium Salt-Based Monomers

Biimidazolium salt (BIm)-based monomers were prepared via combination of 1-vinyl imidazole and dibromoalkane with different spacer chain lengths (as shown in Scheme 1). Their structures were characterized using  $^1\text{H}$ -,  $^{13}\text{C}$ -NMR, ESI-MS, and EA. The results demonstrated that all these BIm-based monomers were synthesized with acceptable yield. Likewise,  $^1\text{H}$ -NMR spectra of these monomers were conducted in different deuterium solvents (as shown in Figures 1–3, the detail of  $^1\text{H}$ -NMR are shown in the supplementary materials). A prominent characteristic can be found that the signals associated with the C-2 proton in the imidazolium ring in all these BIm-based monomers can be observed clearly when the measurements were conducted in  $\text{DMSO-}d_6$ . Nevertheless, these peaks cannot be observed when the measurements were conducted in deuterated water. To get more information about this feature of BIm-based monomers, deuterated water was added into  $\text{DMSO-}d_6$  in the measurement process. As illustrated in Figure 1, an obvious decrease in chemical shift can be seen after the addition of  $\text{D}_2\text{O}$ . When more  $\text{D}_2\text{O}$  was added, the signal associated with the C-2 proton almost disappeared. These results indicate that the C-2 proton of imidazolium ring is very active, and can exchange with the protons of polar solvents, such as water and methanol. However, the signal associated with the C-2 proton could also be observed in  $\text{D}_2\text{O}$  when the measurement was conducted immediately after the solution was prepared (Figure 3), which indicates that the exchanging process is not very quickly. In brief, it could be confirmed that C-2 proton of the imidazolium ring in the above BIm-based monomers are active enough to form hydrogen-bond interactions with polar solvents, such as water and methanol.



**Scheme 1.** Synthetic route of biimidazolium-based ionic liquids. ( $n = 2, 3, 5$ ).

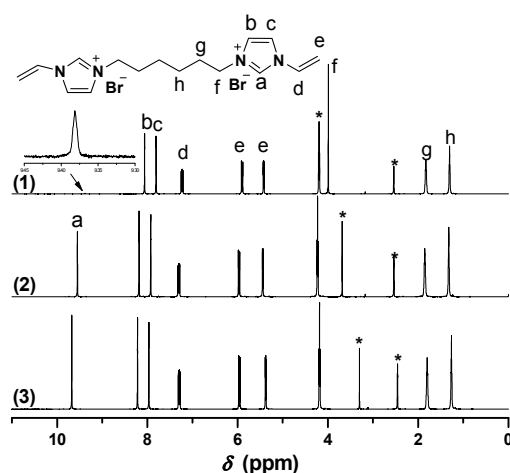


**Figure 1.**  $^1\text{H}$ -NMR of  $[\text{C}_6\text{VIm}]\text{Br}$  in different deuterium solvents. ((1) 0.6 mL  $\text{DMSO-}d_6$  + 0.1 mL  $\text{D}_2\text{O}$ , 30 min later; (2)  $\text{DMSO-}d_6$  + 0.05 mL  $\text{D}_2\text{O}$ , immediately; (3) 0.6 mL  $\text{DMSO-}d_6$ ).

\* The peak is ascribed to the solvent.

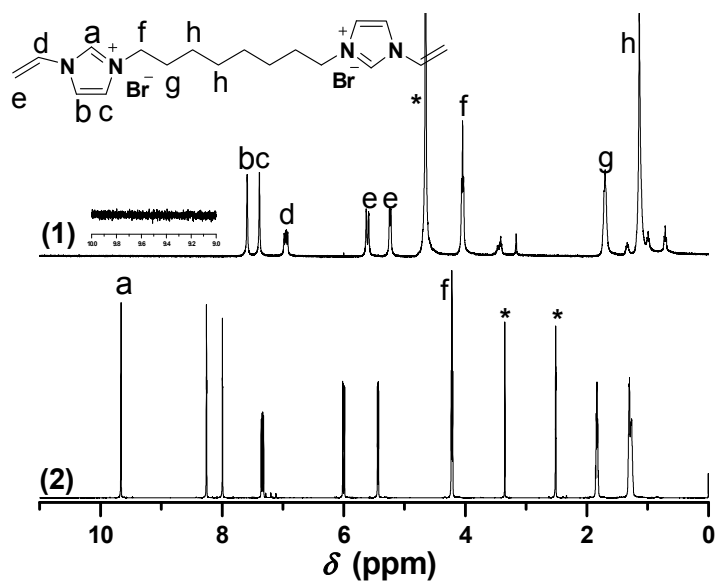


**Figure 2.**  $^1\text{H-NMR}$  of  $[\text{C}_8\text{VIm}]\text{Br}$  in different deuterium solvents. ((1)  $\text{D}_2\text{O}$ ; (2)  $\text{DMSO-}d_6$ ).

\* The peak is ascribed to the solvent.

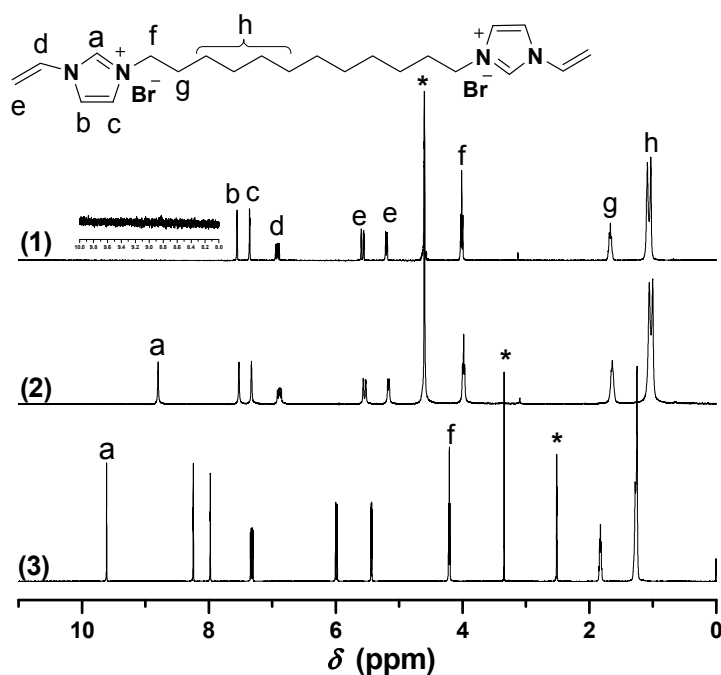
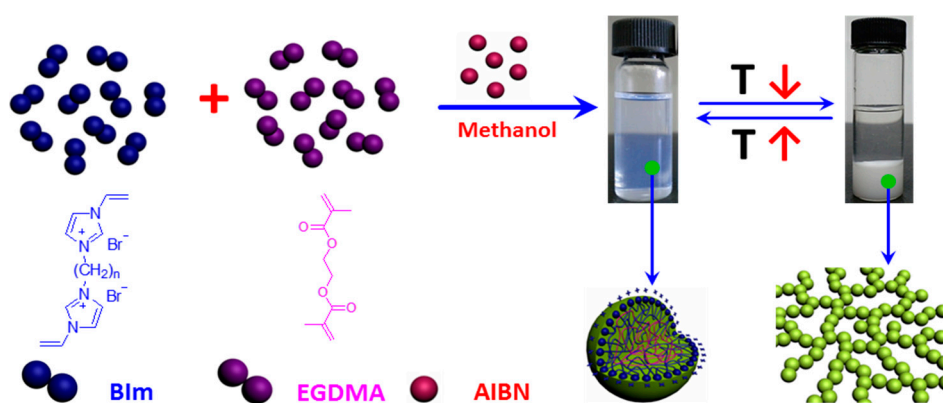


**Figure 3.**  $^1\text{H-NMR}$  of  $[\text{C}_{12}\text{VIm}]\text{Br}$  in different deuterium solvents. ((1)  $\text{D}_2\text{O}$ , 30 min later; (2)  $\text{D}_2\text{O}$ , immediately; (3)  $\text{DMSO-}d_6$ ). \* The peak is ascribed to the solvent.

## 2.2. Characterization of *BIm* Salt-Based Nanogels and Their Thermo-Responsive Behavior

In our previous studies [29], it has been demonstrated that the structure of IL-based monomers play a key role in the one-step synthesis of highly cross-linked nanogel. When 1-vinyl-3-(2-methoxy-2-oxyl ethyl) imidazolium chloride was copolymerized under the same conditions, the obtained particles in the submicrometer precipitated from the solvent during the polymerization process. However, when 1,4-butanediyl-3,3'-bis-1-vinyl imidazolium bromide was copolymerized, the as-prepared nanogels

could be well-dispersed in the solution and transform reversibly to precipitation or macrogel formation in methanol with the temperature changes [28]. Notably, novel thermo-responsive nanogel will promisingly be obtained by introducing hydrogen-bond interactions into IL-based nanogel. To investigate the relationship between the structure and thermo-response of nanogels in more detail, BIm-based monomers were copolymerized with the cross-linkers EGDMA and DVB via convention radical polymerization in selective solvent. As illustrated in Scheme 2, BIm-based monomers ( $n = 6, 8,$  and  $12$ ) can be successfully copolymerized with the cross-linkers to obtain the well-dispersed nanogels in the solution. Additionally, the nanogel solutions were very stable and could be stored without any precipitation for more than several months. The results illustrate that BIm-based monomers can stabilize the nanogels during the polymerization process. More interestingly, these BIm-based nanogels are also thermo-responsive. When the temperature decreases, the nanogels precipitate from the solvent. Inversely, the nanogels could be well-dispersed in the solvent again when the temperature increases. The performance testifies that BIm-based nanogels are of the phase behavior with UCST.



**Scheme 2.** Schematic illustration of one-step synthesis of BIm-based nanogels, and their thermo-responsive behavior with temperature changes.

The cross-linking copolymerization with different monomers and feed ratio were conducted. Then, the size and  $\zeta$ -potential of BIm-based nanogels were checked using dynamic light scattering (DLS), and the results are summarized in Table 1. It indicates that BIm-based nanogels with the size less than 160 nm can be facily prepared via the one-step synthesis. Moreover, for the  $[C_6VIm]Br + EGDMA$  series, hydrodynamic diameters decreased from 160 to 70 nm on decreasing the cross-linking. The particles would precipitate from the solution when the feed ratio of BIm-based monomer to EGDMA was less than 3:1. A similar trend can be observed when DVB is used as the cross-linker. This performance is reasonable because BIm-based monomers play the role of stabilizer in the cross-linking copolymerization process. Likewise [26–29], hydrodynamic diameters of these BIm-based nanogels are in a wide distribution except Entry 5. In addition, all nanogels are positively charged, and the higher feed ratio of BIm-based monomers will enhance the  $\zeta$ -potential on the surface of nanogels. As a result, positive  $\zeta$ -potential can improve the stability of nanogels in the solution due to electrostatic repulsion. These results strongly demonstrate that the one-step synthesis is an effective and universal method for the preparation of imidazolium-based nanogels.

**Table 1.** Size, PDI, and  $\zeta$ -potential of nanogels prepared with different feed ratios in methanol.

| Entry | Monomer and Cross-Linker        | Feed Ratio (Molar Ratio) <sup>a</sup> | D <sub>h</sub> (nm) | PDI  | $\zeta$ -Potential (mV) |
|-------|---------------------------------|---------------------------------------|---------------------|------|-------------------------|
| 1     | [C <sub>6</sub> VIm]Br + EGDMA  | 1:1                                   | precipitated        | -    | -                       |
| 2     | [C <sub>6</sub> VIm]Br + EGDMA  | 3:1                                   | 159                 | 0.28 | 11.5                    |
| 3     | [C <sub>6</sub> VIm]Br + EGDMA  | 5:1                                   | 137                 | 0.26 | 12.4                    |
| 4     | [C <sub>6</sub> VIm]Br + EGDMA  | 10:1                                  | 103                 | 0.43 | 14.1                    |
| 5     | [C <sub>6</sub> VIm]Br + EGDMA  | 15:1                                  | 71                  | 0.09 | 18.1                    |
| 6     | [C <sub>8</sub> VIm]Br + EGDMA  | 10:1                                  | 125                 | 0.36 | 13.5                    |
| 7     | [C <sub>12</sub> VIm]Br + EGDMA | 10:1                                  | 148                 | 0.45 | 11.9                    |
| 8     | [C <sub>6</sub> VIm]Br + DVB    | 3:1                                   | 111                 | 0.39 | 14.6                    |
| 9     | [C <sub>6</sub> VIm]Br + DVB    | 5:1                                   | 88                  | 0.29 | 16.2                    |
| 10    | [C <sub>6</sub> VIm]Br + DVB    | 10:1                                  | 47                  | 0.33 | 17.1                    |

<sup>a</sup>: [C<sub>n</sub>VIm]Br to cross-linker; D<sub>h</sub>: hydrodynamic diameter; PDI: polydispersion. - No data are available.

The morphology of as-prepared nanogels was also examined using scanning electron microscopy (SEM). As shown in Figure 4, spherical particles with sizes of less than 200 nm can be clearly observed. Most of the particles are smaller than the corresponding hydrodynamic diameter determined by DLS (Table 1). It is because that DLS provides the data for the particles swollen in the solution, whereas SEM presents the images of dried particles. It can also be seen from Figure 4a–i that BIm-based nanogels are liable to aggregate in the dry state, which results in enlargement of some particles.

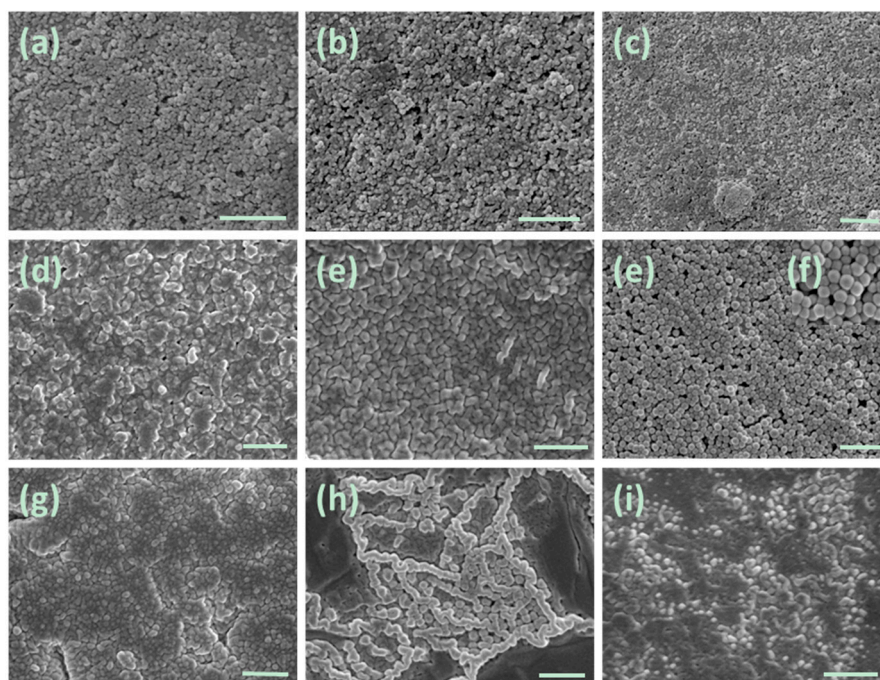


**Figure 4.** SEM images of BIm-based nanogels. ((a) [C<sub>6</sub>VIm]Br:EGDMA = 10:1; (b) [C<sub>8</sub>VIm]Br:EGDMA = 10:1; (c) [C<sub>12</sub>VIm]Br:EGDMA = 10:1; (d) [C<sub>6</sub>VIm]Br:EGDMA = 15:1; (e) [C<sub>6</sub>VIm]Br:EGDMA = 5:1; (f) [C<sub>6</sub>VIm]Br:EGDMA = 3:1; (g) [C<sub>6</sub>VIm]Br:DVB = 3:1; (h) [C<sub>6</sub>VIm]Br:DVB = 5:1; (i) [C<sub>6</sub>VIm]Br:DVB = 10:1). The scale bar is 500 nm.

To put more light on the relationship between the structure of BIm-based monomers and the thermo-response of nanogels, phase transform behavior of BIm-based nanogels were also investigated using turbidimetry and DLS. Figure 1 shows the temperature dependence of turbidity and diameters for 5.0 wt % nanogel solutions in methanol. All these nanogel solutions are blue, opalescent, and translucent above a certain temperature, and suddenly turned cloudy below the above temperature. For example, the transmittance of nanogel solution ( $[\text{C}_6\text{VIm}]\text{Br}:\text{EGDMA} = 5:1$ , Figure 1a) is above 80% at the temperature 18 °C. Nonetheless, the transmittance dropped promptly to below 10% when the temperature decreases to 13 °C. The discrete transition that occurred within a narrow temperature change indicates that nanogels are thermosensitive particles with an upper critical solution temperature (UCST). The thermosensitive behavior of nanogels was also confirmed by DLS measurements. The hydrodynamic diameter ( $D_h$ ) of nanogels increased rapidly from below 100 nm to micrometer level in the same temperature range. These results reveal that free nanogels were suddenly desolvated to form large aggregates, and precipitated from the solvent below UCST.

Though BIm-based nanogels with different constitutions can present thermo-responsive behavior in methanol, marogel cannot be observed in the present system even at lower temperature (−20 °C). This performance is very different from that of nanogels with short spacer in BIm-based monomer [28]. It is probably because that H-bond interaction between imidazolium ring and methanol is not strong enough in the present system. From Figure 5c,d, It can also be inferred that more  $[\text{C}_6\text{VIm}]\text{Br}$  in the feed will obviously enhance the UCST of the corresponding nanogel when using DVB as the cross-linker.

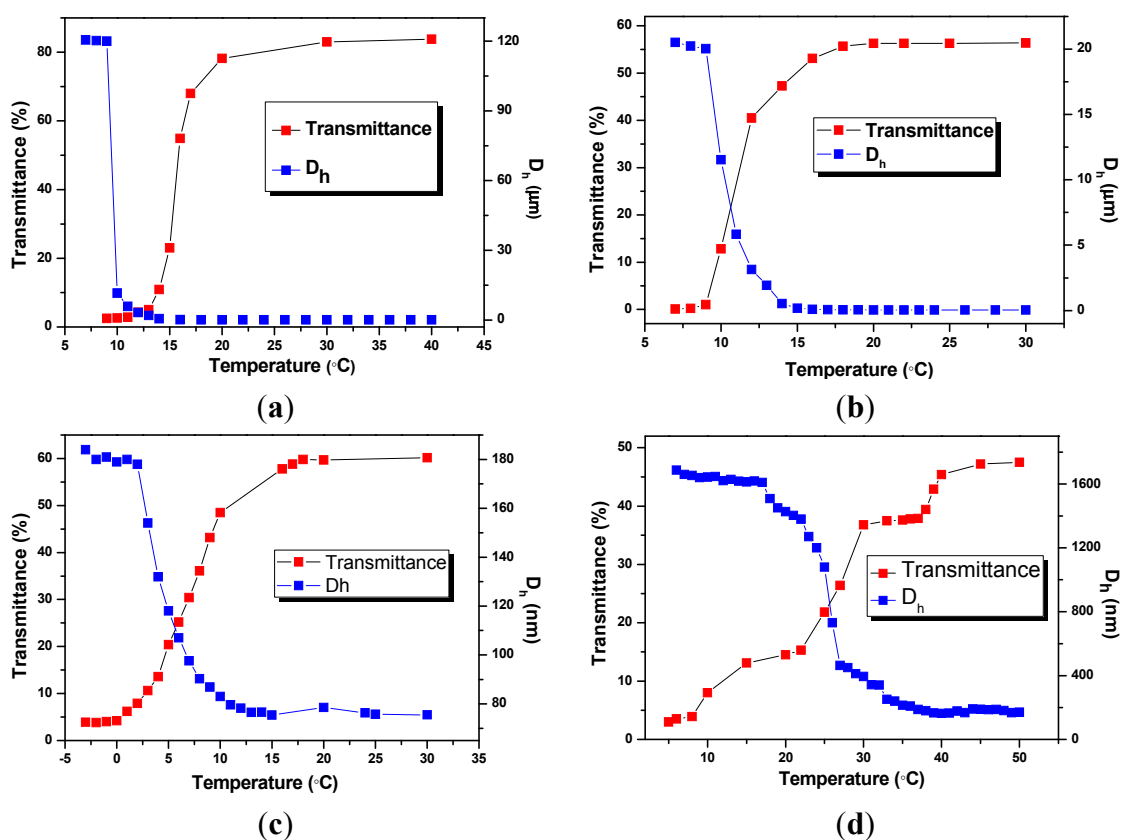


**Figure 5.** Temperature dependence of transmittance at 500 nm and hydrodynamic diameters ( $D_h$ ) for 5 wt % nanogel in methanol. ((a)  $[\text{C}_6\text{VIm}]\text{Br}:\text{EGDMA} = 5:1$ ; (b)  $[\text{C}_6\text{VIm}]\text{Br}:\text{EGDMA} = 10:1$ ; (c)  $[\text{C}_6\text{VIm}]\text{Br}:\text{DVB} = 3:1$ ; (d)  $[\text{C}_6\text{VIm}]\text{Br}:\text{DVB} = 10:1$ ).

FTIR spectra of the as-prepared nanogels with different BIm-based monomers and cross-linkers are indicated in Figure 6. Some typical peaks attributed to BIm-based ILs and EGDMA/DVB copolymers can be clearly recognized, such as aromatic benzene ring ( $1646, 1500\text{ cm}^{-1}$ , stretching vibration), aromatic imidazolium ring ( $1454, 1180\text{ cm}^{-1}$  stretching vibration), carbonyl group ( $1730\text{ cm}^{-1}$ , stretching vibration), *etc.* Especially, the peak ascribed to the carbon-carbon double bond ( $1582\text{ cm}^{-1}$ , stretching vibration) in the vinyl group of the monomers disappeared. These results demonstrate the formation of BIm-based copolymers. Thermo-stabilities of the as-prepared nanogels were measured using thermogravimetric analysis (TGA). As illustrated in Figure 7, these BIm-based copolymers are stable below  $250\text{ }^{\circ}\text{C}$ , which may be due to their highly cross-linked structure. Therefore, they can be used in some catalytic reactions at high temperatures. What is more, the weight loss before  $150\text{ }^{\circ}\text{C}$  is because of the absorbed water or solvents, and they enhanced with the increase of BIm-based monomers in the feed.

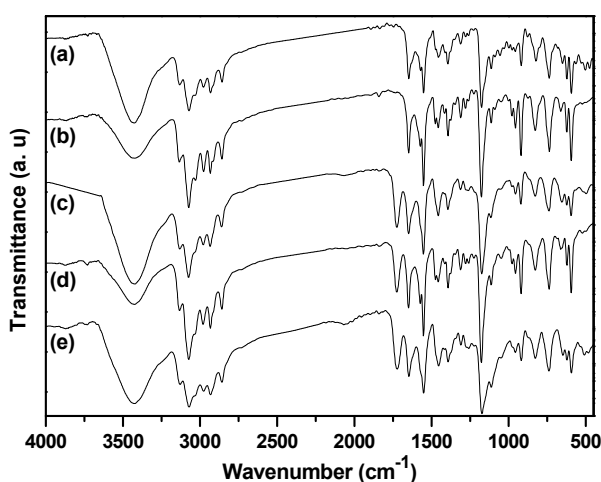


**Figure 6.** FTIR spectra of BIm-based nanogels with different monomers and feed ratio. ((a)  $[\text{C}_6\text{VIm}]\text{Br}:\text{DVB} = 5:1$ ; (b)  $[\text{C}_6\text{VIm}]\text{Br}:\text{DVB} = 10:1$ ; (c)  $[\text{C}_6\text{VIm}]\text{Br}:\text{EGDMA} = 10:1$ ; (d)  $[\text{C}_8\text{VIm}]\text{Br}:\text{EGDMA} = 10:1$ ; (e)  $[\text{C}_{12}\text{VIm}]\text{Br}:\text{EGDMA} = 10:1$ ).

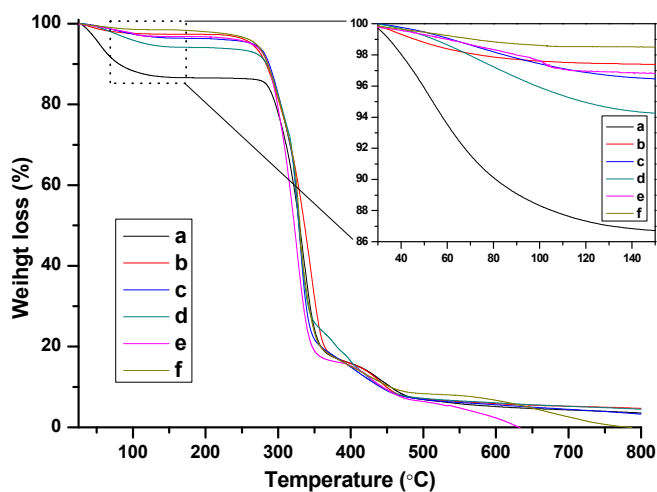


**Figure 7.** TG curves of BIm-based nanogels with different monomers and feed ratio. ((a)  $[\text{C}_6\text{VIm}]\text{Br}:\text{EGDMA} = 15:1$ ; (b)  $[\text{C}_8\text{VIm}]\text{Br}:\text{EGDMA} = 10:1$ ; (c)  $[\text{C}_6\text{VIm}]\text{Br}:\text{EGDMA} = 5:1$ ; (d)  $[\text{C}_6\text{VIm}]\text{Br}:\text{EGDMA} = 10:1$ ; (e)  $[\text{C}_{12}\text{VIm}]\text{Br}:\text{DVB} = 10:1$ ; (f)  $[\text{C}_6\text{VIm}]\text{Br}:\text{DVB} = 3:1$ ).



IR spectroscopy is an useful method to study the interactions between ILs and solvents, as well as the formation/disruption of H-bonds [30,31]. It has been reported that the IR spectra of dried imidazolium-based ILs present a prominent absorption band at  $3058\text{ cm}^{-1}$ , which is attributed to the C–H stretching vibration for  $\text{C–H}\cdots\text{X}^-$  [32]. Upon uptake of water or other proton solvents, the peaks associated with the aromatic C–H stretching vibration and the C–H stretching vibration of the  $\text{C–H}\cdots\text{X}^-$  shift to higher wavenumbers. According to Pimentel and McClellan [33], the stretching mode of an A–H moiety shifts to higher frequencies upon H-bond disruption. Infrared spectra of dried BIm-based nanogels and the ones containing little methanol are shown in Figure 8. According to the reports, the peaks at  $3130$  and  $3063\text{ cm}^{-1}$  in the dried sample are attributed to the aromatic C–H stretching vibration and the C–H stretching vibration of  $\text{C–H}\cdots\text{Br}^-$ , respectively. However, the according peaks in the sample containing methanol shift to higher wavenumbers, as compared to the dried samples. This performance illustrates the disruption/diminution of the H-bond between the imidazolium ring and  $\text{Br}^-$ , probably due to the presence of residual methanol. That is, in the presence of methanol, H-bond interactions between BIm-based nanogels and methanol may produce, and the H-bond network between nanogels and methanol results in precipitation of nanogels from the solution. However, the above H-bond interactions are weak, and can be disrupted at higher temperature. As a result, reversible phase transform is produced due to the formation/disruption of H-bond network in different temperature ranges.

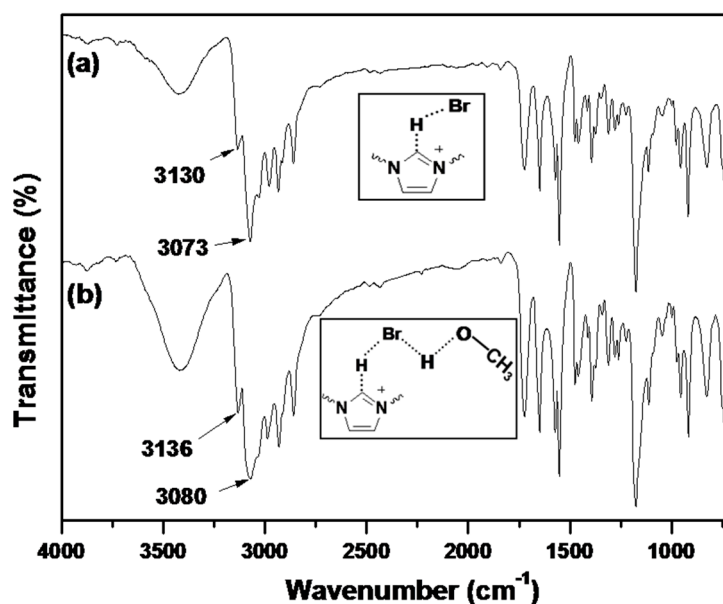


**Figure 8.** FTIR spectra of poly(EGDMA-co-[C<sub>6</sub>VIm]Br). ((a) dried sample; and (b) the sample containing methanol).

### 2.3. Catalysis Performance of BIm Salt-Based Nanogels for the Cycloaddition Reaction

Catalytic performance of various BIm-based nanogels for the cycloaddition reactions of  $\text{CO}_2$  to epichlorohydrin (ECH) was investigated, and the results are summarized in Table 2. It can be seen that all these nanogel catalysts presented high activity ( $>87\%$ ) and selectivity ( $>89\%$ ). Higher reaction temperature,  $\text{CO}_2$  pressure and imidazolium salt content in the nanogels benefit to improve the yield of cyclic carbonate. Under the optimal conditions, both the activity and the selectivity of cyclic carbonate can achieve as high as 100% when catalyzed by the nanogel with the feed ratio of EGDMA to [C<sub>6</sub>VIm]Br

of 10:1. The results above elucidated the high activity of BIm-based nanogel catalysts. It is presumably due to their nanostructure providing larger specific surface area and be dispersed easily in the substrate and product. Compared with the IL-based nanogels [26,27,34–36], the catalytic activity of biimidazolium-based nanogels is lower, especially the selectivity of cyclocarbonate. Only when the reaction temperature increased as high as 160 °C, the highest yield and selectivity could be achieved.

**Table 2.** Performance of BIm-based nanogel catalyst for the cycloaddition reaction of CO<sub>2</sub> with ECH in different temperature <sup>a</sup>.

| Entry | Catalyst <sup>b</sup> | Temperature (°C) | CO <sub>2</sub> (MPa) | Yield (%) | Selectivity (%) |
|-------|-----------------------|------------------|-----------------------|-----------|-----------------|
| 1     | 3:1                   | 160              | 3                     | 99.7      | 89.0            |
| 2     | 5:1                   | 160              | 3                     | 99.8      | 93.0            |
| 3     | 10:1                  | 160              | 3                     | 100       | 100             |
| 4     | 15:1                  | 160              | 3                     | 100       | 96.4            |
| 5     | 5:1                   | 120              | 3                     | 87.7      | 99.3            |
| 6     | 5:1                   | 140              | 3                     | 96.1      | 96.1            |
| 7     | 5:1                   | 150              | 3                     | 99.5      | 99.2            |
| 8     | 5:1                   | 160              | 2                     | 95.7      | 97.3            |
| 9     | 5:1                   | 160              | 5                     | 99.7      | 100             |

<sup>a</sup>: Reaction condition: ECH 3 mL, nanogel 0.1 g, time 6 h; <sup>b</sup>: feed ratio of [C<sub>6</sub>VIm]Br to EGDMA.

### 3. Experimental Section

Carbon dioxide with a purity of 99.99% was provided from a commercial source. 1-Vinylimidazole (VIm, 98%), 1,6-dibromohexane, 1,8-dibromooctane, 1,12-dibromododecane, ethylene glycol dimethacrylate (EGDMA, 98%), and divinyl benzene (DVB, 98%) were brought from Aladdin Reagent Co. (Shanghai, China). The inhibitor in VIm, EGDMA, and DVB were removed through distillation on vacuum. Azobisisobutyronitrile (AIBN) was purchased from Tianjing Chemical Reagent Company (Tianjing, China), and recrystallized from methanol before use. Other reagents, such as 2,6-Di-tert-butyl-4-methylphenol, methanol, diethyl ether, and acetone were A.R. grade and used without further purification.

Fourier transform infrared (FT-IR) spectra were recorded on a DIGIL FTS3000 spectrophotometer (DIGILAB, Randolph, MA, USA) using KBr tablets. <sup>1</sup>H- and <sup>13</sup>C-NMR spectra were recorded on a Bruker AM 400 MHz spectrometer (Bruker, Faellanden, Switzerland) at 25 °C. Thermogravimetric analyses (TGA) were measured on a Perkin Elmer TG/TGA 6300 (Perkin E Itachi instruments, Norwalk, USA) at a heating rate of 10 °C min<sup>-1</sup>. Differential scanning calorimetry (DSC) measurements were recorded on a DSC 822e thermal analysis system (Mettler Toledo Instruments Inc., Greifensee, Switzerland) at a heating rate of ±1 °C/min with nitrogen protected (80 mL min<sup>-1</sup>). The morphology of nanogels was observed by scanning electron microscopy (SEM, JSM 67001F JEOL, Tokyo, Japan), and the samples were prepared by dispersing the dried nanogels in methanol under sonication at room temperature. The X-ray diffraction analysis was recorded on a Philips X'Pert using Cu K $\alpha$  radiation at 40 kV (Rigaku, Tokyo, Japan). Dynamic light scattering (DLS) measurements were performed at 25 °C and a scattering angle of 90° on a commercial laser light scattering (ALV/SP-125) equipped with an ALV-5000 multi- $\tau$  digital time correlator and ADLAS DPY425 solid-state laser (output power = 22 mW at  $\lambda$  = 632.8 nm) (ALV-GmbH, Langen, Germany). Zeta potential values were calculated according to

Smolochowski equation and each sample was analyzed in triplicate (Malvern instruments Ltd., Worcestershire, UK). The upper critical solution temperature (UCST) of thermo-sensitive nanogels was measured by turbidimetry at 500 nm using a spectrophotometer (UV-VIS Spectrometer, Lambda 20, Perkin-Elmer, Waltham, MA, USA). The elemental analyses are measured directly without any additives using a Vario EL Cube (Elementar, Hanau, Germany), and mass spectroscopy were performed using water as the solvent without additives on a micrOTOF-QII mass spectrometer (Bruker Daltonics, Billerica, MA, USA).

*1,6-Hexanediyl-3,3'-bis-1-vinyl imidazolium bromide* ( $[C_6VIm]Br$ ) 1-vinyl imidazole (5.18 g, 55 mmol) and 1,6-dibromohexane (2.79 g, 22 mmol) were dissolved in methanol (50 mL) in a round-bottom flask fitted with a condenser and  $N_2$  bubbler. Subsequently, the mixture was stirred at 80 °C for 48 h under a nitrogen atmosphere. After then, the reaction mixture was precipitated from diethyl ether (150 mL), and recrystallized twice from diethyl ether. The products were dried under vacuum for 24 h at R.T.  $[C_6VIm]Br$  was obtained as white solid. Yield: 71%.  $[C_6VIm]Br$ :  $^1H$ -NMR ( $D_2O$ , 400 MHz, ppm): 7.57 (1H, s); 7.37 (1H, s); 6.93 (1H, m); 5.60 (1H, d); 5.22 (1H, d); 4.04 (2H, t); 1.70 (2H, s); 1.17 (2H, s).  $^1H$ -NMR (DMSO, 400 MHz, ppm): 9.66 (1H, s); 8.24 (1H, t); 7.99 (1H, t); 7.33 (1H, m); 5.99 (1H, m); 5.43 (1H, m); 4.22 (2H, t); 1.83 (2H, d); 1.31 (2H, s).  $^{13}C$ -NMR (DMSO, 100 MHz, ppm): 135.36, 128.88, 123.31, 119.23, 109.04, 49.02, 28.80, 24.77. ESI-MS ( $m/z$ ): calcd. for  $C_{16}H_{24}N_4Br_2$ : 432.2, found: 432.2. Elemental analysis (%): Calculated: C, 44.46; H, 5.60; N, 12.96; Br, 36.98. Found: C, 42.94; H, 5.36; N, 12.50; Br, 39.20. M.P.: 219 °C.

*1,8-Octanediyl-3,3'-bis-1-vinyl imidazolium bromide* ( $[C_8VIm]Br$ ) 1-vinyl imidazole (0.94 g, 10 mmol) and 1,8-dibromooctane (1.36 g, 5 mmol) were dissolved in methanol (50 mL) in a round-bottom flask fitted with a condenser and  $N_2$  bubbler. Subsequently, the mixture was stirred at 80 °C for 48 h under a nitrogen atmosphere. After then, the reaction mixture was precipitated from diethyl ether (150 mL), and recrystallized twice from diethyl ether. The products were dried under vacuum for 24 h at R.T. Yield: 27%.  $[C_8VIm]Br$ :  $^1H$ -NMR ( $D_2O$ , 400 MHz, ppm): 8.868 (1H, s); 7.598 (1H, d); 7.398 (1H, d); 6.969 (1H, m); 5.605 (1H, m); 5.255 (1H, m); 4.057 (2H, t); 1.724 (2H, m); 1.152 (4H, s).  $^{13}C$ -NMR ( $D_2O$ , 100 MHz, ppm): 128.39; 122.97; 119.61; 109.47; 50.07; 29.15; 28.00; 25.37. ESI-MS ( $m/z$ ): calcd. for  $C_{18}H_{28}N_4Br_2$ : 460.26, Found: 460.1. Elemental analysis (%): Calculated: C, 47.15; H, 6.16; N, 12.23; Br, 34.46. Found: C, 47.40; H, 5.73; N, 11.87; Br, 35. Mp: 173–175 °C.

*1,12-Dodecanediyl-3,3'-bis-1-vinyl imidazolium bromine* ( $[C_{12}VIm]Br$ ) 1-vinyl imidazole (0.94 g, 10 mmol) and 1,12-dibromododecane (1.64 g, 5 mmol) were dissolved in methanol (50 mL) in a round-bottom flask fitted with a condenser and  $N_2$  bubbler. Subsequently, the mixture was stirred at 80 °C for 48 h under a nitrogen atmosphere. After then, the reaction mixture was precipitated from diethyl ether (150 mL), and recrystallized twice from diethyl ether. The products were dried under vacuum for 24 h at R.T. Yield: 60%.  $[C_{12}VIm]Br$ :  $^1H$ -NMR ( $D_2O$ , 400 MHz, ppm): 8.80 (1H, s); 7.53 (1H, s); 7.33 (1H, s); 6.88 (1H, m); 5.55 (1H, m); 5.17 (1H, d); 3.98 (2H, t); 1.64 (2H, s); 1.03 (8H, d).  $^{13}C$ -NMR ( $D_2O$ , 100 MHz, ppm): 134.21, 128.34, 122.94, 119.51, 109.34, 50.06, 28.68, 25.39. ESI-MS ( $m/z$ ): calcd. for  $C_{22}H_{36}N_4Br_2$ : 516.36, Found: 516.2. Elemental analysis (%): Calculated: C, 51.17; H, 7.03; N, 10.85; Br, 30.95. Found: C, 50.34; H, 6.86; N, 10.62; Br, 32.18. Mp: 134.2 °C.

*Cross-linking copolymerization of [C<sub>n</sub>VIm]Br and EGDMA* Biimidazolium (BIm)-based nanogels were prepared by conventional radical copolymerization of [C<sub>n</sub>VIm]Br and cross-linkers using AIBN as initiator in selective solvents. The following example describes the typical synthesis of nanogel using 500 mol % [C<sub>n</sub>VIm]Br based on EGDMA. This protocol is representative of all nanogel syntheses. [C<sub>6</sub>VIm]Br (2.12 g, 4.9 mmol), EGDMA (0.194 g, 0.98 mmol), and AIBN (0.021 g, 0.13 mmol) were dissolved in methanol (50 mL), and the mixture was stirred at 70 °C for 48 h. After then, the mixture was precipitated from diethyl ether (150 mL), and the products were washed with THF, and diethyl ether, respectively. The products were dried under vacuum for 24 h at 50 °C. (Yield: 62.5%).

All the cycloaddition reactions were carried out in a 50 mL stainless steel reactor with magnetic stirrer and automatic temperature control system. After appropriate amounts of epoxides and catalyst were charged into, CO<sub>2</sub> was introduced in, and the pressure was kept constantly till the reaction was completed. Then the reactor was heated to desired temperature. After the proper reaction time, the reactor was cooled to 0 °C by immersing into iced water. Then CO<sub>2</sub> was released through a cold trap with DMF to capture the reactants and products entrained by CO<sub>2</sub>. The catalyst was recovered by filtration. The resulting filtrate together with the absorbent was analyzed by gas chromatography (Shimadzu GC-7A, Kyoto, Japan). The retention time of the products were compared with available authentic standards. The cyclic carbonates were characterized on a Bruker 400 MHz NMR spectrometer using CDCl<sub>3</sub> as solvent at room temperature (data not shown).

#### 4. Conclusions

In summary, thermo-responsive polymeric nanogels can be facilely prepared via one-step cross-linking copolymerizing of ethylene glycol dimethacrylate/divinylbenzene and biimidazolium-based monomers, 1,*n*-butanediyl-3,3'-bis-1-vinyl imidazolium bromides ([C<sub>n</sub>VIm]Br, *n* = 6, 8, 12) in selective solvents. The diameters of these nanogels are tunable via the feed ratio of BIm-monomers and the cross-linkers. It is also found that these BIm-based nanogels are thermo-responsive, and display reversible, temperature-driven phase transition in methanol. These nanogels are characterized by FTIR, TG, and SEM. Moreover, BIm-based nanogels are effective catalysts for CO<sub>2</sub> cycloaddition reactions with epoxides. Such attributes make them a robust material platform suitable for a wide range of applications.

#### Supplementary Materials

Supplementary materials can be accessed at: <http://www.mdpi.com/1420-3049/20/09/17378/s1>.

#### Acknowledgments

The authors are grateful for the financial support given by the National Natural Science Foundation of China (Project No. 21164008, 21474080) and Natural Science Foundation of Gansu Province (Project No. 1208RJZA167). Program for Changjiang Scholars and Innovative Research Team in University of Ministry of Education of China (Project No. IRT1177), Scientific and Technical Innovation Project of Northwest Normal University (nwnu-kjcxgc-03-63). We also thank M. Jiang, P. Yao, and D. Chen (Fudan University) for DLS, and FTIR measurements.

## Author Contributions

Yubing Xiong conceived and designed the experiments; Jingjiang Liu and Jing Zhang performed the experiments; Yong Zuo and Rongmin Wang analyzed the data; Yubing Xiong and Jing Zhang wrote the paper.

## Conflicts of Interest

The authors declare no conflict of interest.

## References

1. Parvulescu, V.I.; Hardacre, C. Catalysis in ionic liquids. *Chem. Rev.* **2007**, *107*, 2615–2665.
2. Han, D.; Row, K.H. Recent applications of ionic liquids in separation technology. *Molecules* **2010**, *15*, 2405–2426.
3. Dominguez de Maria, P. “Nonsolvent” Applications of ionic liquids in biotransformations and organocatalysis. *Angew. Chem. Int. Ed.* **2008**, *47*, 6960–6968.
4. Welton, T. Room-temperature ionic liquids. Solvents for synthesis and catalysis. *Chem. Rev.* **1999**, *99*, 2071–2083.
5. Skoda-Földes, R. The use of supported acidic ionic liquids in organic synthesis. *Molecules* **2014**, *19*, 8840–8884.
6. Armand, M.; Endres, F.; MacFarlane, D.R.; Ohno, H.; Scrosati, B. Ionic-liquid materials for the electrochemical challenges of the future. *Nat. Mater.* **2009**, *8*, 621–629.
7. Lu, J.; Yan, F.; Texter, J. Advanced applications of ionic liquids in polymer science. *Prog. Polymer Sci.* **2009**, *34*, 431–448.
8. Nishimura, N.; Ohno, H. 15th anniversary of polymerised ionic liquids. *Polymer* **2014**, *55*, 3289–3297.
9. Mecerreyes, D. Polymeric ionic liquids: Broadening the properties and applications of polyelectrolytes. *Prog. Polymer Sci.* **2011**, *36*, 1629–1648.
10. Erdmenger, T.; Guerrero-Sanchez, C.; Vitz, J.; Hoogenboom, R.; Schubert, U.S. Recent developments in the utilization of green solvents in polymer chemistry. *Chem. Soc. Rev.* **2010**, *39*, 3317–3333.
11. Antonietti, M.; Kuang, D.B.; Smarsly, B.; Zhou, Y. Ionic liquids for the convenient synthesis of functional nanoparticles and other inorganic nanostructures. *Angew. Chem. Int. Ed.* **2004**, *43*, 4988–4992.
12. Ando, T.; Kohno, Y.; Nakamura, N.; Ohno, H. Introduction of hydrophilic groups onto the ortho-position of benzoate anions induced phase separation of the corresponding ionic liquids with water. *Chem. Commun.* **2013**, *49*, 10248–10250.
13. Fukumoto, K.; Ohno, H. LCST-Type Phase Changes of a Mixture of Water and Ionic Liquids Derived from Amino Acids. *Angew. Chem. Int. Ed.* **2007**, *46*, 1852–1855.
14. Ribot, J.C.; Guerrero-Sanchez, C.; Hoogenboom, R.; Schubert, U.S. Thermoreversible ionogels with tunable properties via aqueous gelation of an amphiphilic quaternary ammonium oligoether-based ionic liquid. *J. Mater. Chem.* **2010**, *20*, 8279–8284.
15. Ribot, J.; Guerrero-Sanchez, C.; Hoogenboom, R.; Schubert, U. Aqueous gelation of ionic liquids: Reverse thermoresponsive ion gels. *Chem. Commun.* **2010**, *46*, 6971–6973.

16. Kohno, Y.; Deguchi, Y.; Ohno, H. Ionic liquid-derived charged polymers to show highly thermoresponsive LCST-type transition with water at desired temperatures. *Chem. Commun.* **2012**, *48*, 11883–11885.
17. Ueki, T. Stimuli-responsive polymers in ionic liquids. *Polymer J.* **2014**, *46*, 646–655.
18. Yuan, J.; Mecerreyes, D.; Antonietti, M. Poly(ionic liquid)s: An update. *Prog. Polymer Sci.* **2013**, *38*, 1009–1036.
19. Kohno, Y.; Saita, S.; Men, Y.; Yuan, J.; Ohno, H. Thermoresponsive polyelectrolytes derived from ionic liquids. *Polymer Chem.* **2015**, *6*, 2163–2178.
20. Kohno, Y.; Arai, H.; Ohno, H. Ionic liquid/water mixtures: From hostility to conciliation. *Chem. Commun.* **2011**, *47*, 4772–4774.
21. Anderson, K.; Rodríguez, H.; Seddon, K.R. Phase behaviour of trihexyl (tetradecyl) phosphonium chloride, nonane and water. *Green Chem.* **2009**, *11*, 780–784.
22. Kagimoto, J.; Nakamura, N.; Kato, T.; Ohno, H. Novel thermotropic gels composed of only ions. *Chem. Commun.* **2009**, 2405–2407.
23. Fukaya, Y.; Sekikawa, K.; Murata, K.; Nakamura, N.; Ohno, H. Miscibility and phase behavior of water-dicarboxylic acid type ionic liquid mixed systems. *Chem. Commun.* **2007**, 3089–3091.
24. Yuan, J.; Soll, S.; Drechsler, M.; Muller, A.H.E.; Antonietti, M. Self-assembly of poly(ionic liquid)s: Polymerization, mesostructure formation, and directional alignment in one step. *J. Am. Chem. Soc.* **2011**, *133*, 17556–17559.
25. Saita, S.; Kohno, Y.; Nakamura, N.; Ohno, H. Ionic liquids showing phase separation with water prepared by mixing hydrophilic and polar amino acid ionic liquids. *Chem. Commun.* **2013**, *49*, 8988–8990.
26. Xiong, Y.B.; Wang, H.; Wang, R.M.; Yan, Y.F.; Zheng, B.; Wang, Y.P. A facile one-step synthesis to cross-linked polymeric nanoparticles as highly active and selective catalysts for cycloaddition of CO<sub>2</sub> to epoxides. *Chem. Commun.* **2010**, *46*, 3399–3401.
27. Xiong, Y.B.; Wang, Y.J.; Wang, H.; Wang, R.M. A facile one-step synthesis to ionic liquid-based cross-linked polymeric nanoparticles and their application for CO<sub>2</sub> fixation. *Polymer Chem.* **2011**, *2*, 2306–2315.
28. Xiong, Y.B.; Liu, J.J.; Wang, Y.J.; Wang, H.; Wang, R.M. One-step synthesis of thermosensitive nanogels based on highly cross-linked poly(ionic liquid)s. *Angew. Chem. Int. Ed.* **2012**, *51*, 9114–9118.
29. Xiong, Y.B.; Wang, Y.J.; Wang, H.; Wang, R.M.; Cui, Z. Novel one-step synthesis to cross-linked polymeric nanoparticles as highly active and selective catalysts for cycloaddition of CO<sub>2</sub> to epoxides. *J. Appl. Polymer Sci.* **2012**, *123*, 1486–1493.
30. Wulf, A.; Fumino, K.; Ludwig, R. Spectroscopic evidence for an enhanced anion-cation interaction from hydrogen bonding in pure imidazolium ionic liquids. *Angew. Chem. Int. Ed.* **2010**, *49*, 449–453.
31. Peppel, T.; Roth, C.; Fumino, K.; Paschek, D.; Kockerling, M.; Ludwig, R. The influence of hydrogen-bonding defects on the properties of ionic liquids. *Angew. Chem. Int. Ed.* **2011**, *50*, 6661–6665.
32. Sun, B.; Jin, Q.; Tan, L.; Wu, P.; Yan, F. Trace of the interesting “V”-shape dynamic mechanism of interaction between water and ionic liquids. *J. Phys. Chem. B* **2008**, *112*, 14251–14259.
33. Pimentel, G.C.; McClellan, A.L. *The Hydrogen Bond*; Freeman: San Francisco, CA, USA, 1960; pp. 348–363.

34. Xie, Y.; Zhang, Z.F.; Jiang, T.; He, J.L.; Han, B.X.; Wu, T.B.; Ding, K.L. CO<sub>2</sub> cycloaddition reactions catalyzed by an ionic liquid grafted onto a highly cross-linked polymer matrix. *Angew. Chem. Int. Ed.* **2007**, *119*, 7393–7396.
35. Peng, J.J.; Deng, Y.Q. Cycloaddition of carbon dioxide to propylene oxide catalyzed by ionic liquids. *New J. Chem.* **2001**, *25*, 639–641.
36. Sun, J.; Cheng, W.G.; Fan, W.; Wang, Y.H.; Meng, Z.Y.; Zhang, S.J. Reusable and efficient polymer-supported task-specific ionic liquid catalyst for cycloaddition of epoxide with CO<sub>2</sub>. *Catal. Today* **2009**, *148*, 361–367.

*Sample Availability:* Samples of [C<sub>6</sub>VIm]Br and [C<sub>8</sub>VIm]Br are available from the authors.

© 2015 by the authors; licensee MDPI, Basel, Switzerland. This article is an open access article distributed under the terms and conditions of the Creative Commons Attribution license (<http://creativecommons.org/licenses/by/4.0/>).